Journal of Power Sources 235 (2013) 243–250

Contents lists available at SciVerse ScienceDirect

Journal of Power Sources

journal homepage: www.elsevier.com/locate/jpowsour

Monolithic quasi-solid-state dye-sensitized solar cells based on iodine-free polymer gel electrolyte

Yaoguang Rong, Xiong Li, Guanghui Liu, Heng Wang, Zhiliang Ku, Mi Xu, Linfeng Liu, Min Hu, Ying Yang, Meili Zhang, Tongfa Liu, Hongwei Han*

Michael Grätzel Center for Mesoscopic Solar Cells, Wuhan National Laboratory for Optoelectronics, School of Optical and Electronic Information, Huazhong University of Science and Technology, Wuhan, Hubei 430074, PR China

HIGHLIGHTS

- Monolithic dye-sensitized solar cell using iodine-free electrolyte is developed.
- The electrolyte presents high conductivity and non-absorption characters.
- A high efficiency of up to 6.97% has been obtained.
- The effect of additives on the device has been thoroughly investigated.

ARTICLE INFO

Article history:
Received 2 November 2012
Received in revised form
16 January 2013
Accepted 12 February 2013
Available online 19 February 2013

Keywords:
Monolithic
Dye-sensitized solar cell
Iodine-free
Quasi-solid-state
Polymer gel electrolyte
High efficiency

ABSTRACT

A monolithic quasi-solid-state dye-sensitized solar cell assembled with an iodine-free polymer gel electrolyte (IFGE) and a printable mesoscopic carbon counter electrode was developed. The IFGE was prepared by employing an ionic liquid (1,2-dimethyl-3-propylimidazolium iodide, DMPII) as the charge transfer intermediate and a polymer composite as the gelator without the addition of iodine, exhibiting high conductivity and non-absorption characters. The dependences of ionic conductivity and photovoltaic performance on DMPII concentration in the IFGE were investigated. An overall power conversion efficiency (PCE) of 4.94% could be obtained for the IFGE with an ionic conductivity of 21.18 mS cm^{-2} under 100 mW cm^{-2} AM 1.5 illumination. The effects of additives lithium iodide (LiI) and *N*-methylbenzimidazole (NMBI) on the photovoltaic performance of the devices were also investigated. An optimal efficiency of up to 6.97% was obtained and the results were substantiated by incident photon-to-current conversion efficiency (IPCE) spectrum, electrochemical impedance spectroscopy (EIS) and intensity modulated photovoltage spectroscopy (IMVS) measurements.

1. Introduction

Growing attention has been concentrated on the utilization of renewable energies such as photovoltaic in order to deal with the problems of energy crisis and global warming. Since Prof. M. Grätzel made breakthrough in 1991 [1], dye-sensitized solar cells (DSSCs) have been expected to be a potential candidate of the next-generation solar cells due to the advantages of high efficiency and low-cost fabricating procedures [2–4].

In general, typical DSSCs have a sandwich structure with two transparent conducting glass substrates, between which comprises of a nanoporous TiO_2 working electrode, a liquid-state electrolyte containing iodide and triiodide ions as redox couple, and a platinized counter electrode to collect electrons and catalyze the redox couple regeneration reaction [3,4]. Up to now, the power conversion efficiency (PCE) of DSSCs based on this structure and liquid-state electrolyte has reached to 11.5% [5]. However, potential problems caused by liquid electrolytes, such as the leakage and volatilization of the liquid solvent, desorption and degradation of the dyes, and the corrosion of the platinum counter electrode have blocked the commercial application of DSSCs. Thus, solid-state and quasi-solid-state electrolytes, such as polymer gel electrolyte [6–9], organic hole-transporting materials [10,11], inorganic p-type semiconductors [12], and solvent-free polymer electrolyte [13,14] have been proposed as alternatives to the liquid electrolytes. However, the efficiency of DSSCs using such solid-state materials

* Corresponding author.
E-mail address: hongwei.han@mail.hust.edu.cn (H. Han).

0378-7753/$ – see front matter © 2013 Elsevier B.V. All rights reserved.
http://dx.doi.org/10.1016/j.jpowsour.2013.02.032

was still unsatisfactory compared with that achieved by the liquid electrolyte, ascribed to the low charge transport ability of the solid-state electrolyte and poor contact of the electrolyte with the dye coated TiO_2 surface [4,15].

Among various alternatives for liquid electrolytes, polymer gel electrolyte (PGE) incorporating iodide/triiodide redox couple appears to have superior properties in terms of ionic conductivity and cell performance [6–9]. For the PGE, the liquid electrolyte was trapped in a polymer matrix and, thereby, the solvent evaporation was inhibited. Although the polymer network may hinder the ion transfer, the ions can move freely in the channels of polymer network which benefits the ionic conductivity of a PGE. In the past decade, many different PGEs have been developed to fabricate quasi-solid-state DSSCs, and a PCE of over 9% has been obtained [16]. However, introducing the iodine into the electrolytes for improving their conductivity decreased the stability and performance of DSSCs due to the sublimation of iodine and the incident light absorption by iodine [17–19]. Moreover, iodine also causes hurdles for manufacturing large-scale solar modules, ascribing to its corrosive nature to metals. Besides, the noble metal such as platinum and F-doped tin oxide (FTO) glass substrates used for the counter electrodes, which account for most of the DSSC-fabrication cost, are still an issue for the wide applications of DSSCs. To realize further cost reductions, the use of FTO glass and noble metal for the counter electrodes should be minimized and abundantly available catalytic materials need to be developed.

Monolithic DSSCs, fabricated on a single FTO glass substrate with three layers of a nanoporous TiO_2 working electrode layer, an insulating/scattering layer and a carbon counter electrode layer, offer the prospect of lower material cost and require a simpler manufacturing process compared with traditional DSSCs [20–23]. Since all the layers could be fabricated by screen-printing, not only the thicknesses of the electrodes could be controlled precisely, but also the distance between working and counter electrode becomes controllable and reproducible, which makes it accessible for monolithic DSSCs to obtain reproducible photovoltaic performance. For large-scale monolithic DSSC modules, the adjacent unit cells could be directly connected in series by the carbon counter electrodes avoiding printing extra metal grids [20,23,24]. All these values make it a promising design for commercial applications.

Herein, we report a high efficiency monolithic quasi-solid-state DSSC assembled with an iodine-free polymer gel electrolyte (IFGE) and a printable mesoscopic carbon counter electrode. The IFGE employs an ionic liquid (1,2-dimethyl-3-propylimidazolium iodide, DMPII) as the charge transfer intermediate and the source of redox couple, a polymer composite of poly(ethylene oxide)/poly (vinylidenefluoride-*co*-hexafluoropropylene) (PEO/PVDF-HFP) as the polymeric host and acetonitrile as the solvent. The dependences of ionic conductivity and photovoltaic performance on the DMPII concentration in the IFGE were investigated. It should be noted that although many papers have shown the improvement in DSSC performance using electrolytes that combine ionic liquid with several different types of materials, only a few papers present the investigation of an electrolyte based solely on the ionic liquid as the source of redox couple [25–28]. To further improve the performance of the devices, lithium iodide (LiI) and *N*-methyl-benzimidazole (NMBI) were incorporated into the IFGE as additives. It was found that the addition of LiI and NMBI to the IFGE caused significant increases in the short-circuit current density (J_{sc}) and open-circuit voltage (V_{oc}), and achieved an optimal efficiency of up to 6.97%, the highest ever reported efficiency for a quasi-solid-state DSSC fabricated with carbon counter electrode in the absence of iodine [28].

2. Experimental

2.1. Materials

Poly(ethylene oxide) (PEO, M_W = 600,000 g mol^{-1}), poly(-vinylidene fluoride-co-hexafluoro propylene) ((PVDF-HFP), M_W = 100,000 g mol^{-1}), lithium iodide (LiI, 99.9%), *N*-methyl-benzimidazole (NMBI, 99%) and acetonitrile (ACN, AR) were purchased from Sigma–Aldrich. 1,2-dimethyl-3-propylimidazolium iodide (DMPII) was synthesized according to the literature [29]. Colloidal anatase TiO_2 paste (PASOL HPW-18NR) was obtained from JGC Catalysts and Chemicals Ltd. (Japan). The ZrO_2 paste and carbon paste were prepared as we reported previously [21,30].

2.2. Preparation of the IFGE

For the preparation of the IFGE, DMPII was dissolved in 8 ml ACN to obtain a solution with a molar concentration ranging from 0.05 M to 1.2 M, and stirred for about 20 min. Then 1.25 g (20 wt% relative to the amount of ACN) polymer composite with PEO/PVDF-HFP = 2:3 wt% was added into the solution. The solution was stirred for 24 h at 70 °C to obtain the desired homogeneous transparent IFGE. For the modification of the IFGE, LiI and NMBI were added into the electrolyte if necessary. For comparison, an iodine-based gel electrolyte (IGE) containing 0.6 M DMPII, 0.1 M LiI, 0.1 M I2 and 0.45 M NMBI in ACN with 20% polymer composite was also prepared. The electrolyte solutions were kept under stirring for about 3 h before each measurement to assure the electrolyte homogeneous.

2.3. Assembly of the monolithic DSSCs

The structure of the monolithic DSSCs is shown in Fig. 1. Based on this structure, electrodes of 20 cells (4 × 5) were constructed on a single glass substrate. After the pre-treatment of the glass substrate (TEC-15, Pilkington) including the laser structuring of the FTO layer and the washing of the glass, a dense TiO_2 layer was deposited on the glass substrate by spray pyrolysis deposition with

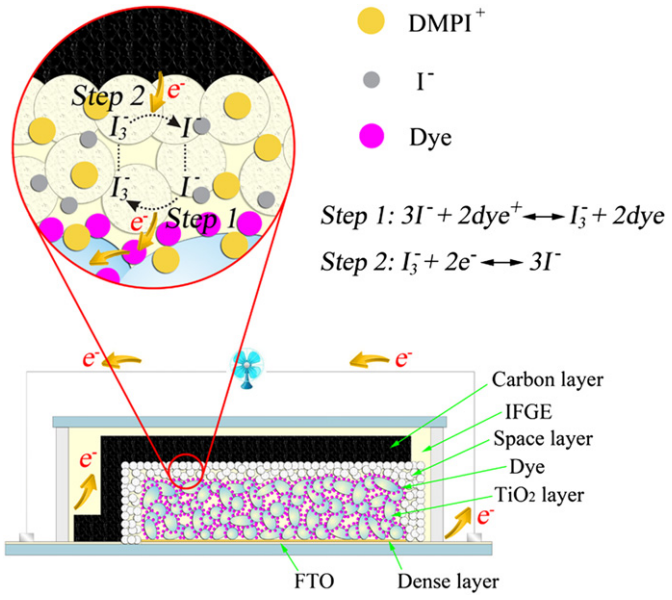

Fig. 1. The structure and charge transfer mechanism of a typical iodine-free monolithic quasi-solid-state DSSC based on an ionic liquid and a printable mesoscopic carbon counter electrode.

di-isopropoxytitanium bis(acetyl acetonate) solution. Then a 12 μm nanoporous TiO_2 layer, a 3 μm ZrO_2 layer, and a 50 μm carbon layer were screen-printed on the substrate layer by layer. The TiO_2 layer and ZrO_2 layer were sintered at 500 °C for 30 min, and the carbon layer was sintered at 400 °C for 30 min. After cooling to 80 °C, the substrate was immersed in the acetonitrile and tert-butyl alcohol mixed solution (volume ratio, 1:1) containing 0.5 mM N719 at room temperature for about 24 h. After dye application, the glass substrate was cut into 20 individuals for further processing. A thin layer of the gel electrolyte was spread on the top of the CCE using a razor blade, and then a glass sheet was placed onto the gel film. To obtain a complete nanopore filling for the gel electrolyte, a vacuum condition was applied [31]. Finally, an adhesive was employed to fix and seal the cell.

2.4. Instrumentation and measurements

2.4.1. Impedance spectroscopy measurement

The ionic conductivity (σ) of the IFGE was measured using the Pt/IFGE/Pt sandwich type electrode structure. A potentiostat (EG&G, M2273, USA) was applied to measure the impedance (Nyquist plot) of the IFGE. A perturbation voltage of 10 mV was applied over the frequency range 40 Hz to 1 MHz. The ionic conductivity was calculated by the following equation:

$$\sigma = \frac{L}{AR_b} \quad (1)$$

Here L is the thickness of the IFGE and A is the area of the electrode. The resistance (R_b) is taken at the intercept of the Nyquist plot with the real axis.

2.4.2. Photovoltaic characterization

Photocurrent density–voltage characteristics were measured with a Keithley 2400 source meter under illumination with an Oriel solar simulator composed of a 1000 W xenon arc lamp and AM 1.5 G filters. Light intensity was calibrated with a normative silicon cell. The area of cell is 0.8 cm × 0.8 cm and the active area for the photocurrent density–voltage characteristics is fixed to 0.13 cm^2 with a mask.

2.4.3. Electrochemical impedance spectroscopy (EIS) measurement

The EIS measurements were carried out by using a potentiostat (EG&G, M2273) with applying bias of the open circuit voltage (V_{oc}) under dark condition. The frequency range analyzed was 0.02 Hz to 10^6 Hz with ac amplitude of 10 mV.

2.4.4. Incident photon-to-current conversion efficiency (IPCE) measurement

The IPCE measurement was measured using a 150 W xenon lamp (Oriel) fitted with a mono-chromator (Cornerstone 74004) as a monochromatic light source. The illumination spot size was chosen to be slightly smaller than the active area of the DSSC test cells. IPCE photocurrents were recorded under short-circuit conditions using a Newport 2931-C power meter. The monochromatic photon flux was quantified by means of a calibrated silicon photodiode.

2.4.5. Intensity-modulated photovoltage spectroscopy (IMVS) measurement

The IMVS measurement was carried out using high-intensity green LEDs (530 nm) driven by a ZAHNER Xpot frequency response analyzer. The LED provided both the dc and ac components of the illumination. The ac light intensities were modulated (±8%) by modulating the voltage applied to the LED with sinusoidal waves in the frequency range from 0.02 to 200 Hz for IMVS. The dc illumination intensity was varied by controlling the voltage applied to the LED. The dc and ac light intensities were measured with a calibrated photodiode. All experiments were performed in an earthed Faraday dark-box to eliminate electrical noise at low light intensities.

2.4.6. UV–vis spectra analysis

The absorption measurement of the IFGE and IGE was performed by a UV–vis Spectrophotometer (Lambda 950, PerkinElmer). The electrolyte was placed between two glass substrates to assemble a sandwich structure cell. The thickness of the electrolyte was about 100 μm.

3. Results and discussion

3.1. Structure and working principle

The structure of a typical monolithic DSSC and the charge transfer mechanism for the IFGE based monolithic DSSC is illustrated in Fig. 1. Based on the design of a triple layer structure, all the three layers of TiO_2 layer, ZrO_2 layer and carbon layer are constructed on a single conducting glass substrate. The porous ZrO_2 layer functions as a scattering layer on the top of the working electrode and a space insulator to separate dyed TiO_2 layer and carbon layer electrically. The mesoscopic carbon counter electrode (CCE) with large porosity and surface area favors the penetration of the electrolyte from the top of the carbon layer to the TiO_2 layer and provides a large catalyst area for the reduction of I_3^- to I^-. For the traditional I^-/I_3^- liquid electrolyte based DSSCs, iodide and iodine in the electrolyte exist in the form of polyiodides such as I_3^- or I_5^- and an efficient transport of iodide and triiodide in the electrolyte is necessary for good performance of the devices because the oxidized state of the dye (dye^+) should be reduced by I^- ions efficiently after the electrons from the excited state of the dye are injected into the conduction band of TiO_2 under illumination [4]. Here for the IFGE based monolithic DSSCs, I^- ions accomplish the charge transfer in the electrolyte through reacting with oxidized dye to generate I_3^- firstly (Step 1), and then the I_3^- ions return to I^- species by obtaining electrons from the CCE (Step 2). According to our result, we suggest that iodide anion based ionic liquid (DMPII) in the IFGE can provide sufficient I^- for the regeneration of the oxidized dye under illumination. Meanwhile, in the case of polymer composite in the IFGE, the intimate interactions between $DMPI^+$ and oxygen atoms of the polyethylene oxide units would cause more free mobile I^- ions, and promote the regeneration of the oxidized dye, correspondingly accelerate the charge carrier transfer.

3.2. Conductivity of the IFGE

For DSSCs, the overall power conversion efficiency (PCE) is heavily dependent upon the mobility of the redox couple and consequently on the ionic conductivity of the electrolyte [7,27,32]. Since, the IFGE employed DMPII as the charge transfer intermediate, the conductivity of the electrolyte and the performance of the devices are significantly affected by the DMPII concentration of the electrolyte. The dependence of ionic conductivity on the DMPII concentration in the electrolyte is shown in Fig. 2 and the inset shows the photographs of IFGE containing 0.4 M DMPII from top (a) and side (b). Clearly, with an increase in DMPII concentration from 0.05 M to 0.4 M, the conductivity of the IFGE increases sharply from 5.54 mS cm^{-1} to 21.18 mS cm^{-1}. When DMPII concentration is higher than 0.4 M, only a slight increase in the conductivity is observed.

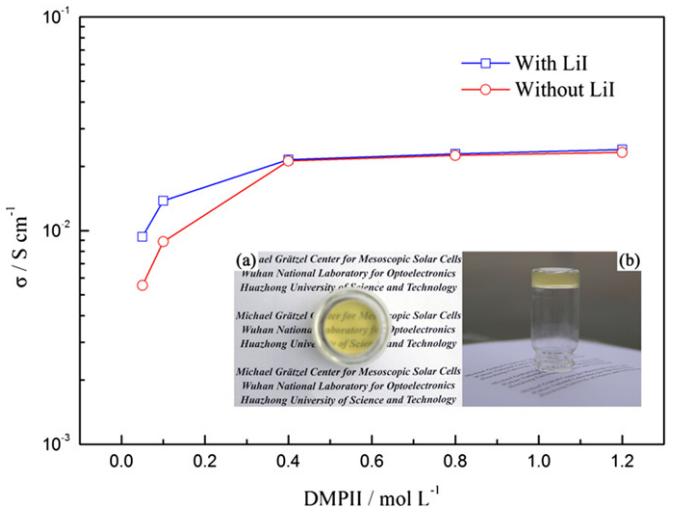

Fig. 2. Dependence of the ionic conductivity on DMPII concentration of the IFGE with (square) and without LiI (circle). The inset shows the photographs of IFGE containing 0.4 M DMPII from top (a) and side (b).

For the PEO/PVDF-HFP polymer composite based quasi-solid-state electrolytes, the ionic conductivity is governed by the transport of I^- ions. The intimate interactions between $DMPI^+$ and oxygen atoms of the polyethylene oxide units cause free mobile I^- ions. At low concentration range, the increase in the conductivity with increasing DMPII concentration is caused by the increase of charge carriers, since the conductivity of the IFGE is a function of the number of charge carriers in the polymer gel electrolyte. At high concentration range, excessive DMPII merely increases the charge carrier concentration since coordination interaction has already been saturated, thus resulting in a low increasing rate in the conductivity. Besides, a high DMPII concentration increases the viscosity of the electrolyte and reduces the segmental motion of the polymer chains, thus decreases the conductivity of the IFGE.

3.3. The influence of DMPII concentration on the performance of devices

Table 1 summarizes the photovoltaic parameters of devices assembled with IFGE containing different amounts of DMPII. As can be seen, the short-circuit current density (J_{sc}) firstly increases from 4.89 mA cm^{-2} to 10.20 mA cm^{-2} when DMPII concentration increases from 0.05 M to 0.4 M, whereas a further increase of DMPII concentration from 0.4 M to 1.2 M does not lead to obvious increase in J_{sc}. This change in J_{sc} is in agreement with the change trends of the conductivity of the IFGE as shown in Fig. 2. Because low conductivity causes rate-determining of charge transportation and increasing the series resistance, it is supposed that the increase in J_{sc} when DMPII concentration is lower than 0.4 M is attributed to enhanced ionic conductivity of the IFGE, which provides more efficient I^-/I_3^- transportation in the electrolyte and decreases the series resistance of the device.

For the open-circuit voltage (V_{oc}), it is believed that the addition of imidazolium ionic liquids such as DMPII to the electrolyte could suppress the back electron transfer between the conduction band of the TiO_2 electrode and the triiodide ion in the electrolyte, and obtain a high V_{oc} [33]. However, excessive DMPII added to the electrolyte would also result in a gradual decrease in V_{oc}, which has negative effect on the PCE of the device. The V_{oc}, a difference between Fermi level of TiO_2 and redox potential of electrolyte, is influenced mainly by the molar ratio of I^-/I_3^-. The redox potential (E) can be expressed by Nernst equation:

$$E = E^0 - \frac{RT}{nF}\ln\left(\frac{a_R}{a_o}\right) \quad (2)$$

Here E^0 is the standard electrode potential, R the gas constant, T the absolute temperature, n the electron number per one reaction species, F the Faraday constant, a_R the activity of reduction species and a_o is the activity of oxidation species.

According to Nernst equation, increasing the concentration of reduction species (I^-) would cause a shift of the redox potential to more negative value. Then, the V_{oc} would decrease because the energy gap between the Fermi level of TiO_2 and the redox potential of I^-/I_3^- becomes smaller. Besides, excessive DMPII would also facilitate the charge recombination between the electrons in TiO_2 and I_3^- in the electrolyte, thus reduce the V_{oc} of devices.

Among the results, the device fabricated with IFGE containing 0.4 M DMPII shows the highest conversion efficiency of 4.94%, and V_{oc} of 690.62 mV, J_{sc} of 10.20 mA and FF of 0.70. It should be emphasized that the device in our study works at a high efficiency without the addition of iodine to the quasi-solid-state polymer gel electrolyte. Although it is deduced that trace amounts of iodine are photo-chemically generated from DMPII at the photo-excited dye layer, we found that incorporation of iodine as an initial component of the polymer gel electrolyte is not necessary.

3.4. Additive effect on photovoltaic performance

To optimize the IFGE and achieve a higher efficiency of the device, we incorporated LiI and NMBI into the IFGE as additives. Considering the addition of LiI to the electrolyte would cause an increase in the numbers of charge carriers, we have investigated the influence of 0.1 M LiI on the conductivity of the IFGE containing different amounts of DMPII. The variations of the conductivity for the IFGE with different DMPII concentration after the addition of 0.1 M LiI are shown in Fig. 2. For the IFGE containing 0.05 and 0.1 M DMPII, slight increases in the conductivity are observed when LiI is added. For the IFGE with high DMPII concentration such as 0.4, 0.8 and 1.2 M, the addition of LiI does not lead to obvious improvement in the conductivity.

Table 2 summarizes the device performance parameters obtained for 0.1 M LiI modified IFGE with different DMPII concentration. Generally, the addition of LiI to the IFGE leads to an obvious increase in J_{sc}, and gradual decrease in V_{oc} and FF. The increase in J_{sc} is in agreement with the increase in the ionic conductivity observed for the IFGE with low DMPII concentration (0.05 M and 0.1 M)

Table 1
Photovoltaic performance and ionic conductivity of devices fabricated with IFGE containing different amounts of DMPII.

DMPII/mol L^{-1}	V_{oc}/mV	J_{sc}/mA cm^{-2}	FF	PCE/%	σ/mS cm^{-1}
0.05	706.11	4.89	0.75	2.58	5.54
0.1	697.32	7.06	0.71	3.48	8.87
0.4	690.62	10.20	0.70	4.94	21.18
0.8	667.75	10.20	0.69	4.70	22.50
1.2	654.00	10.85	0.68	4.79	23.23

Table 2
Photovoltaic performance and ionic conductivity of devices fabricated with IFGE containing 0.1 M LiI and different amounts of DMPII.

DMPII/mol L^{-1}	V_{oc}/mV	J_{sc}/mA cm^{-2}	FF	PCE/%	σ/mS cm^{-1}
0.05	557.13	11.99	0.59	3.97	9.35
0.1	565.00	14.17	0.59	4.70	13.77
0.4	625.71	15.20	0.63	5.97	21.49
0.8	591.04	15.22	0.62	5.54	22.86
1.2	586.34	15.25	0.58	5.17	23.92

because of the generation of more charge carriers. However, it should be noted that though the conductivity of the IFGE containing 0.1 M DMPII and 0.1 M LiI is lower than that of the IFGE containing 0.4 M, 0.8 M and 1.2 M DMPII, the J_{sc} of the device is still much higher than that of them. Moreover, for the IFGE with high DMPII concentration (0.4, 0.8 and 1.2 M), though the addition of LiI to the IFGE does not cause obvious improvement in the conductivity, the J_{sc} still increases substantially to over 15.00 mA. These results indicate that the increase in J_{sc} accomplished with the addition of LiI could not only attribute to the improvement of the ionic conductivity of the IFGE. It has been confirmed that the enhanced J_{sc} obtained for LiI modified IFGE based device, compared with pure IFGE based device, was mainly caused by the Li^+ ion rather than by a small increase in the concentration of iodide [34]. Indeed, the effect of lithium ion on the performance of DSSCs has been discussed in many papers. It is supposed that the increase in the J_{sc} should be attributed to the improvement of the electron injection efficiency from the oxidized dye to the TiO_2 conduction band [34–36]. More detailed analysis would be presented in the next section.

Many reports have presented that the intercalation of Li^+ ions into the TiO_2 shifts down the Fermi level of this semiconductor and results in a decrease in the V_{oc} [4,35,36]. For the IFGE based devices, similar results are also found. For the IFGE containing 0.05 M DMPII, the addition of LiI leads to a decrease of ~150 mV in the V_{oc}. For the IFGE containing 0.1 M DMPII, a decrease of ~130 mV was observed. When DMPII concentration is higher than 0.4 M, the influence of LiI on the V_{oc} becomes smaller and exhibits a decrease of ~70 mV.

Fortunately on the whole, the small loss of V_{oc} in the presence of lithium ions is overcompensated by the photocurrent gain, leading to a higher PCE. Among the devices based on LiI modified IFGE, the device fabricated with IFGE containing 0.4 M DMPII and 0.1 M LiI exhibits the highest efficiency of 5.97%. Further increasing DMPII content in the presence of 0.1 M LiI for the IFGE causes a slight decrease in efficiency due to the decrease of V_{oc} and FF, which is similar to the results obtained without LiI.

To enhance the V_{oc} and FF of the devices, *N*-methylbenzimidazole (NMBI) is incorporated into the IFGE. The photocurrent–voltage (*J*–*V*) characteristics of the devices assembled with the electrolytes of $IFGE_{Pure}$, $IFGE_{LiI}$, $IFGE_{NMBI}$, $IFGE_{Both}$ under simulated irradiation (global AM 1.5) are displayed in Fig. 3. The compositions of the modified IFGE and the corresponding parameters of devices are listed in Table 3.

Among LiI and NMBI modified IFGE based monolithic DSSCs, devices using $IFGE_{pure}$ without any additives show the lowest PCE. When LiI is added to the $IFGE_{pure}$, V_{oc} and FF decreased, and J_{sc} increased as mentioned above.

The V_{oc} of the device is significantly increased by ~45 mV when NMBI is added, whereas the J_{sc} involving $IFGE_{NMBI}$ is slightly lower than that of $IFGE_{pure}$. In a comparison between the electrolytes of $IFGE_{LiI}$ and $IFGE_{NMBI}$, the $IFGE_{NMBI}$ based device shows a V_{oc} much higher (~110 mV) and a J_{sc} lower than that of device based on $IFGE_{LiI}$. The device based on the electrolyte $IFGE_{Both}$, containing both LiI and NMBI, displays about the same V_{oc} as that of device with $IFGE_{pure}$. The J_{sc} is somewhat lower as compared with that of $IFGE_{LiI}$, but still much higher than that of $IFGE_{pure}$. Besides, the addition of NMBI into $IFGE_{pure}$ and $IFGE_{LiI}$ also leads to a remarkable improvement in FF. In the case of the modification, the device based on $IFGE_{both}$ shows the highest PCE of 6.97% with the J_{sc} of 14.12, V_{oc} of 681.46 mV, and FF of 0.72.

3.5. Influence of additives on IPCE spectra and injection efficiency

In order to evaluate the origin of variation in photocurrent brought about by the addition of LiI to the electrolyte. We analyze

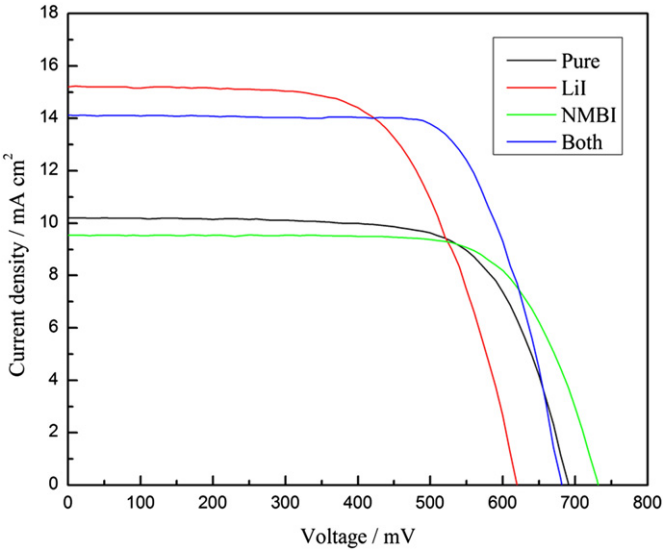

Fig. 3. *J*–*V* curves of devices assembled with different modification IFGE under 100 mW cm^{-2} light irradiation.

the incident photon-to-current conversion efficiency (IPCE) spectra of monolithic DSSCs using the modified IFGE. The incident photon-to-collected-electron conversion efficiency of a DSSC can be defined as

$$\mathrm{IPCE}(\lambda) = \frac{j(\lambda)}{qI_0(\lambda)} = \eta_{\mathrm{lh}}(\lambda)\eta_{\mathrm{inj}}(\lambda)\eta_{\mathrm{col}}\left(\lambda\right)$$

where $j(\lambda)$ is the photocurrent density, q is the elementary charge, $I_0(\lambda)$ is the incident photon flux, $\eta_{lh}(\lambda)$ is the light harvesting efficiency of the sensitized TiO_2 layer (including losses due to the substrate transmission and electrolyte absorption), $\eta_{inj}(\lambda)$ is the efficiency of electron injection from the excited sensitizer to the TiO_2, and the $\eta_{col}(\lambda)$ is the electron collection efficiency. Clearly the IPCE spectrum of a DSSC contains information about light absorption, electron injection, and electron collection.

The IPCE spectra of devices based on the modified IFGE are shown in Fig. 4(a). It could be clearly observed that the addition of LiI to the electrolyte leads to a remarkable improvement in IPCE for both the $IFGE_{Li}$ and $IFGE_{both}$, compared with $IFGE_{pure}$ and $IFGE_{NMBI}$. The result of IPCE test is in agreement with the J_{sc} obtained for the modified IFGE based devices. To eliminate the wavelength-independent variations in the IPCE spectra between samples, such as sample-to-sample variation in substrate transmission or differences in any wavelength-independent component of the electron injection efficiency, normalized IPCE spectra are also given

Table 3
Photovoltaic performance and electrochemical parameters of devices fabricated with IFGE containing different additives.

Electrolyte	Composition
$IFPGE_{pure}$	0.4 M DMPII, 20 wt% Polymer in MeCN
$IFPGE_{Li}$	0.1 M LiI, 0.4 M DMPII, 20 wt% Polymer in MeCN
$IFPGE_{NMBI}$	0.5 M NMBI, 0.45 M DMPII, 20 wt% Polymer in MeCN
$IFPGE_{Both}$	0.1 M LiI, 0.45 M NMBI, 0.4 M DMPII, 20 wt% Polymer in MeCN

Electrolyte	V_{oc}/mV	J_{sc}/mA cm^{-2}	FF	PCE/%	R_{ct1}/Ω	R_{ct2}/Ω
$IFPGE_{pure}$	690.62	10.20	0.70	4.94	5.45	19.97
$IFPGE_{Li}$	625.71	15.20	0.63	5.97	4.16	9.52
$IFPGE_{NMBI}$	733.52	9.52	0.72	5.01	4.79	55.30
$IFPGE_{Both}$	681.46	14.12	0.72	6.97	5.93	17.59

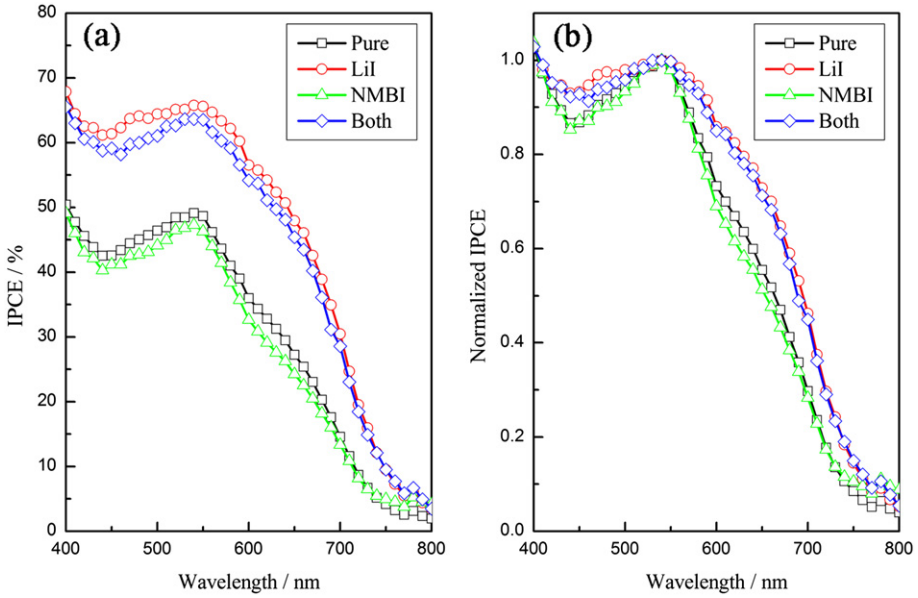

Fig. 4. (a) IPCE spectra of devices assembled with different modification IFGE. (b) IPCE spectra normalized to their respective peaks.

in Fig. 4(b). The remaining differences between the spectra could be due to differences in the wavelength dependence of any of the three partial quantum efficiencies making up the IPCE [36]. Considering the devices are assembled with the sensitized TiO_2 electrodes on the same glass substrate, we assume $\eta_{lh}(\lambda)$ is constant for the devices using different electrolyte. A clear increase in normalized IPCE can be observed at long wavelength, which cannot solely be attributed to increased charge collection efficiency, implying that significant electron injection from nonthermalized sensitizer molecules must occur. On the other hand, the recombination on the TiO_2/dye/electrolyte has been investigated by EIS (see the next section) and the result indicates the enhanced J_{sc} could not be caused by the increase in $\eta_{col}(\lambda)$. Thus, we suppose that the significant improvement in IPCE is attributed to the increase in $\eta_{inj}(\lambda)$, which is in agreement with the result of iodine containing electrolyte based DSSCs as reported [35–39].

In DSSCs, it is found that the electron injection kinetics is strongly dependent upon the concentration of lithium cations in the electrolyte. This dependence is correlated with shifts of the TiO_2 conduction band (CB) energetic as a function of Li^+ concentration. Since the relative energetic of the dye excited state versus the titanium dioxide acceptor state is a key determinant of the dynamics of electron injection in DSSCs, the variations in these energetic impact directly upon device photovoltaic performance [35]. The fastest electron injection dynamics, observed in the presence of 0.1 M Li^+ and 0 M NMBI, yield the highest J_{sc}. However, in this case, the V_{oc} is only 625.71 mV, attributed to the relatively low energy of the TiO_2 acceptor states. Under these conditions, electron injection results in a relatively large loss of free energy. Optimum device performance is obtained with the addition of 0.45 M NMBI to the IFGE, raising the V_{oc} by ~55 mV compared with $IFGE_{LiI}$ and ~45 mV compared with $IFGE_{pure}$. Though a slight decrease in J_{sc} is also observed, indicating lower electron injection efficiency, the loss of photocurrent is more than compensated for by an increase in the TiO_2 Fermi level, resulting in an increase in V_{oc} and higher overall device efficiency. It is reported that the addition of NMBI to the electrolyte would cause the CB to move ~30 mV toward more negative potentials at the same electron concentration in the TiO_2 film, thus enhance the V_{oc} [40].

Optimum device performance is a compromise between achieving a sufficiently large energetic driving force for electron injection to enable electron injection to compete with excited state to ground and raising the TiO_2 CB as high as possible to minimize recombination losses and thus raise cell voltage. It can be viewed as a requirement to minimize the free energy loss associated with electron injection, while still maintaining reasonable high quantum efficiency.

3.6. Influence of additives on charge recombination reaction

In fact, the improvement of the overall efficiency of the device based on $IFGE_{NMBI}$ compared with $IFGE_{LiI}$ should mainly attribute to the increase in the FF rather than the increase in V_{oc}. It has been reported that NMBI could interact with lithium cations and triiodide anions to reduce titania surface coordination and consequently suppress recombination reactions in DSSCs [41,42]. To elucidate the photovoltaic performance of monolithic DSSCs based on the LiI and NMBI modified IFGE, EIS measurements are taken in the dark with applying bias of the open circuit voltage. The Nyquist plots for the monolithic DSSCs based on the $IFGE_{pure}$, $IFGE_{LiI}$, $IFGE_{NMBI}$ and $IFGE_{Both}$ are shown in Fig. 5. Typically, the EIS spectra of DSSCs show three semicircles in the frequency range from 50 mHz to 100 kHz. The ohmic serial resistance (R_s) corresponds to the overall series resistance. The first and second semicircles correspond to the charge-transfer resistances at the counter electrode/electrolyte (R_{ct1}) and the TiO_2/dye/carrier mediator (R_{ct2}) respectively. The third one represents the Warburg diffusion process (R_{diff}) of I^-/I_3^- in the electrolyte. It is generally assumed that the second semicircle represents the recombination process between electrons in TiO_2 and the electrolyte. When the diameter of the middle frequency semicircle is larger, the electron recombination at the TiO_2/dye/electrolyte interface is slighter [43].

It is observed that the high frequency arc radiuses of the devices based on different modified IFGE are almost the same, indicating comparable charge transfer resistances at the CCE/IFGE interfaces. In contrast, significant variations of the middle frequency arc radius are observed. The corresponding parameters obtained from the spectra are summarized in Table 3, and the equivalent circuit is illustrated in the inset of Fig. 5.

Since R_{ct2} of the $IFGE_{LiI}$ based devices (9.52 Ω cm^2) is much smaller than that of $IFGE_{pure}$ based devices (19.97 Ω cm^2), we could conclude that the undesirable low FF obtained for the $IFGE_{LiI}$ is due

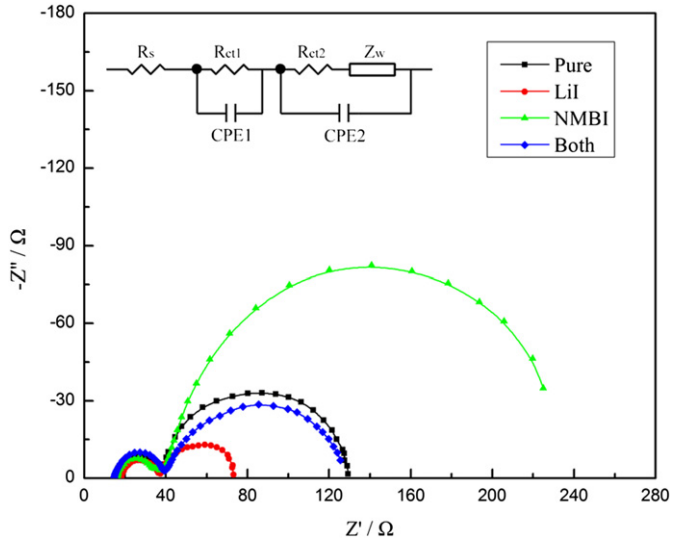

Fig. 5. Electrochemical impedance spectra (EIS) of the devices assembled with different modification IFGE in the dark with applying a bias of the open circuit voltage.

to the increased recombination loss at the TiO_2/dye/electrolyte interface. At the same time, it is confirmed that the increase in the J_{sc} could not attribute to the enhancement of electron collection efficiency. For the $IFGE_{NMBI}$ based device, R_{ct2} (55.30 Ω cm^2) is larger than that of $IFGE_{pure}$ based device, indicating the recombination reactions are effectively suppressed by the addition of NBMI, and the highest V_{oc} of 733.52 mV and FF of 0.72 are obtained. When LiI and NMBI are both added to the IFGE, synergistic effects are observed for the $IFGE_{both}$ based device showing R_{ct2} of 17.59 Ω cm^2 and leading to the highest PCE.

To explore the influence of the modification on the electron lifetime in IFGE based monolithic DSSCs, IMVS spectra of the devices are tested. The IMVS experiment used the same intensity perturbation but measured the periodic modulation of the photovoltage, giving the information of electron lifetime under open-circuit conditions [44]. As shown in Fig. 6, an exponential decrease of τ_e with V_{oc} is clearly observed for all the modified IFGE and the decrease rate is almost constant. It has been concluded that the addition of LiI to the electrolyte would result in a positive shift of the TiO_2 conduction band, thus leads to a decrease of the V_{oc} which has a negative effect on the performance of the device. Herein, it could be found that the addition of LiI does not decrease

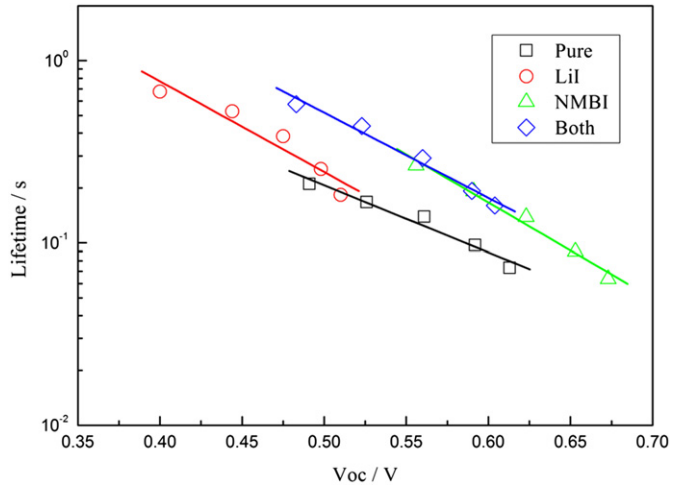

Fig. 6. IMVS spectra of devices assembled with different modification IFGE.

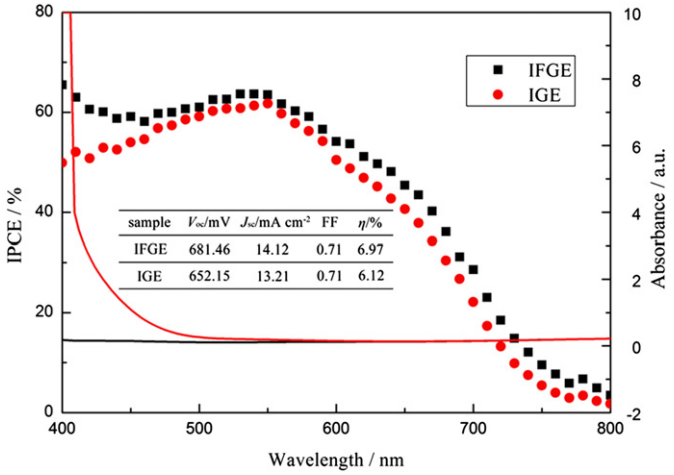

Fig. 7. Absorption spectra of a thin layer of IFGE and IGE confined between two conducting glass substrates (solid line), and IPCE spectra of devices assembled with IFGE and IGE (dot line).

the τ_e, since the $IFGE_{LiI}$ presented a comparable electron lifetime to that of $IFGE_{pure}$ at a given V_{oc}. With NMBI modification, the electron lifetime increased by a factor of ~2.2 at a given V_{oc} for both the $IFGE_{NMBI}$ and $IFGE_{both}$ compared with $IFGE_{pure}$ and $IFGE_{LiI}$. This is due to the strong effect of retarding charge recombination as mentioned in the EIS test. The result is also accorded with the values of V_{oc} obtained in the J–V test.

3.7. Comparison of electrolyte with and without iodine

One of the conditions for the electrolyte to be suitable for use in DSSCs is that the light absorption by the electrolyte in the visible region should be as low as possible [18,45,46]. However, for the traditional iodine-based electrolyte used in DSSCs, the addition of iodine to the electrolyte leads to enhanced light absorption by the carrier mediator existing in the porous dye-coated TiO_2 matrix, which decreases the light-harvesting of the dye molecules.

To investigate the influence of the absorption due to the iodine in the electrolyte on the performance of the devices, we have compared the performances of the devices based on the IFGE and iodine-based gel electrolyte (IGE). The IPCE spectra obtained for the devices using IFGE and IGE, and the absorption spectra of the electrolyte are shown in Fig. 7. The related parameters are listed in the inset. For the IFGE, there is no obvious absorption peak in the range of 400–800 nm. For the IGE, similar result was found in the range of 500–800 nm. But when the light wavelength is below 500 nm, a strong absorption is observed. In this way, for the devices using N719 dye, the absorption spectrum of the IGE overlaps with the N719 dye in the range of 400–450 nm.

The results of the IPCE test are in agreement with the UV–vis measurement of the electrolyte. In the wavelength region of 400–450 nm, the IPCE spectra obtained for the IFGE are clearly higher than that of IGE, which is attributed to the superior character of non-absorption for the IFGE. Besides the undesirable light absorption effect in the short wavelength range, the addition of iodine to the electrolyte may also facilitate the charge recombination between the electrons in TiO_2 and I_3^- in the electrolyte due to the higher concentration of I_3^- in the electrolyte. In this case, the V_{oc} of IGE based device is much lower than that of IFGE based device.

4. Conclusion

In this paper, we have demonstrated an iodine-free polymer gel electrolyte (IFGE) based monolithic DSSCs. The IFGE is prepared in

the absence of iodine and exhibits high conductivity and non-absorption characters. An efficiency of 4.94% is obtained with the IFGE containing DMPII as the sole charge transfer intermediate and source of redox couple. Modified with LiI and NMBI, an optimal efficiency of up to 6.97% is obtained and the effects of additives on the photovoltaic performance of the devices are thoroughly investigated. A significant synergistic effect is observed when NMBI and LiI are used together in the electrolyte, leading to a remarkable improvement of the photovoltaic performance of the device. The increase in short-circuit current density caused by the addition of LiI could be attributed to the increase in the electron injection efficiency of the excited dye, and the improvement of open-circuit voltage and fill factor resulted from the addition of NMBI could be attributed to the longer electron lifetime in the TiO_2 film under open-circuit conditions. This design for DSSCs, incorporating the advantages of monolithic structure and superior properties of iodine-free polymer gel electrolyte, offers the prospect for practical applications of DSSCs and would encourage further improvement of the performance of iodine-free DSSCs.

Acknowledgments

The authors acknowledge the financial support by the Ministry of Science and Technology of China (863, No. SS2013AA50303), the National Natural Science Foundation of China (Grant No. 61106056), the Nature Science Foundation of Hubei Province (2008CDA042), Scientific Research Foundation for Returned Scholars, Ministry of Education of China and the Fundamental Research Funds for the Central Universities (Hust, 2011TS020).

References

[1] B. O'Regan, M. Grätzel, Nature 353 (1991) 737–741.
[2] M.K. Nazeeruddin, A. Kay, I. Rodicio, R.H. Baker, E. Müller, P. Liska, N. Vlachopoulos, M. Grätzel, J. Am. Chem. Soc. 115 (1993) 6382–6390.
[3] M. Gratzel, Nature 414 (2001) 338–344.
[4] A. Hagfeldt, G. Boschloo, L.C. Sun, L. Kloo, H. Pettersson, Chem. Rev. 110 (2010) 6595–6663.
[5] C.Y. Chen, M.K. Wang, J.Y. Li, N. Pootrakulchote, L. Alibabaei, C.H. Ngoc-le, J.D. Decoppet, J.H. Tsai, C. Gratzel, C.G. Wu, S.M. Zakeeruddin, M. Gratzel, ACS Nano 3 (2009) 3103–3109.
[6] P. Wang, S.M. Zakeeruddin, J.E. Moser, M.K. Nazeeruddin, T. Sekiguchi, M. Gratzel, Nat. Mater. 2 (2003) 402–407.
[7] J. Wu, S. Hao, Z. Lan, J. Lin, M. Huang, Y. Huang, L. Fang, S. Yin, T. Sato, Adv. Funct. Mater. 17 (2007) 2645–2652.
[8] Y. Yang, C.H. Zhou, S. Xu, H. Hu, B.L. Chen, J. Zhang, S.J. Wu, W. Liu, X.Z. Zhao, J. Power Sources 185 (2008) 1492–1498.
[9] S. Agarwala, L. Thummalakunta, C.A. Cook, C.K.N. Peh, A.S.W. Wong, L. Ke, G.W. Ho, J. Power Sources 196 (2011) 1651–1656.
[10] U. Bach, D. Lupo, P. Comte, J.E. Moser, F. Weissortel, J. Salbeck, H. Spreitzer, M. Gratzel, Nature 395 (1998) 583–585.
[11] J. Burschka, A. Dualeh, F. Kessler, E. Baranoff, N.L. Cevey-Ha, C.Y. Yi, M.K. Nazeeruddin, M. Gratzel, J. Am. Chem. Soc. 133 (2011) 18042–18045.
[12] Q.B. Meng, K. Takahashi, X.T. Zhang, I. Sutanto, T.N. Rao, O. Sato, A. Fujishima, H. Watanabe, T. Nakamori, M. Uragami, Langmuir 19 (2003) 3572–3574.
[13] H.W. Han, W. Liu, J. Zhang, X.Z. Zhao, Adv. Funct. Mater. 15 (2005) 1940–1944.
[14] Y. Yang, H. Hu, C.H. Zhou, S. Xu, B. Sebo, X.Z. Zhao, J. Power Sources 196 (2011) 2410–2415.
[15] D.M. Li, D. Qin, M.H. Deng, Y.H. Luo, Q.B. Meng, Energy Environ. Sci. 2 (2009) 283–291.
[16] C.-L. Chen, H. Teng, Y.-L. Lee, Adv. Mater. 23 (2011) 4199.
[17] H.X. Wang, X.Z. Liu, Z.X. Wang, H. Li, D.M. Li, Q.B. Meng, L.Q. Chen, J. Phys. Chem. B 110 (2006) 5970–5974.
[18] Z. Yu, M. Gorlov, J. Nissfolk, G. Boschloo, L. Kloo, J. Phys. Chem. C 114 (2010) 10612–10620.
[19] S. Yanagida, Y.H. Yu, K. Manseki, Acc. Chem. Res. 42 (2009) 1827–1838.
[20] A. Kay, M. Grätzel, Sol. Energy Mater. Sol. Cells 44 (1996) 19.
[21] G. Liu, H. Wang, X. Li, Y. Rong, Z. Ku, M. Xu, L. Liu, M. Hu, Y. Yang, P. Xiang, T. Shu, H. Han, Electrochim. Acta 69 (2012) 334–339.
[22] H. Pettersson, T. Gruszecki, R. Bernhard, L. Haggman, M. Gorlov, G. Boschloo, T. Edvinsson, L. Kloo, A. Hagfeldt, Prog. Photovoltaics 15 (2007) 113–121.
[23] H. Pettersson, T. Gruszecki, L.H. Johansson, P. Johander, Sol. Energy Mater. Sol. Cells 77 (2003) 405–413.
[24] Y.G. Rong, X. Li, Z.L. Ku, G.H. Liu, H. Wang, M. Xu, L.F. Liu, M. Hu, P. Xiang, Z.M. Zhou, T. Shu, H.W. Han, Sol. Energy Mater. Sol. Cells 105 (2012) 148–152.
[25] N. Ikeda, K. Teshima, T. Miyasaka, Chem. Commun. (2006) 1733–1735.
[26] G.Q. Wang, L.A. Wang, S.P. Zhuo, S.B. Fang, Y.A. Lin, Chem. Commun. 47 (2011) 2700–2702.
[27] J.N. Chen, T.Y. Peng, K. Fan, J.B. Xia, J. Mater. Chem. 21 (2011) 16448–16452.
[28] C.P. Lee, P.Y. Chen, R. Vittal, K.C. Ho, J. Mater. Chem. 20 (2010) 2356–2361.
[29] P. Bonhote, A.P. Dias, M. Armand, N. Papageorgiou, K. Kalyanasundaram, M. Gratzel, Inorg. Chem. 35 (1996) 1168–1178.
[30] H.W. Han, U. Bach, Y.B. Cheng, R.A. Caruso, C. MacRae, Appl. Phys. Lett. 94 (2009).
[31] H.W. Han, U. Bach, Y.B. Cheng, R.A. Caruso, Appl. Phys. Lett. 90 (2007).
[32] R. Komiya, L.Y. Han, R. Yamanaka, A. Islam, T. Mitate, J. Photochem. Photobiol. A 164 (2004) 123–127.
[33] W. Kubo, S. Kambe, S. Nakade, T. Kitamura, K. Hanabusa, Y. Wada, S. Yanagida, J. Phys. Chem. B 107 (2003) 4374–4381.
[34] P. Wang, S.M. Zakeeruddin, J.E. Moser, M. Gratzel, J. Phys. Chem. B 107 (2003) 13280–13285.
[35] S.E. Koops, B.C. O'Regan, P.R.F. Barnes, J.R. Durrant, J. Am. Chem. Soc. 131 (2009) 4808–4818.
[36] J.R. Jennings, Q. Wang, J. Phys. Chem. C 114 (2010) 1715–1724.
[37] R.Z. Li, D.X. Liu, D.F. Zhou, Y.S. Shi, Y.H. Wang, P. Wang, Energy Environ. Sci. 3 (2010) 1765–1772.
[38] Y.S. Shi, Y.H. Wang, M. Zhang, X.D. Dong, Phys. Chem. Chem. Phys. 13 (2011) 14590–14597.
[39] Q.J. Yu, Y.H. Wang, Z.H. Yi, N.N. Zu, J. Zhang, M. Zhang, P. Wang, ACS Nano 4 (2010) 6032–6038.
[40] Z. Yu, M. Gorlov, G. Boschloo, L. Kloo, J. Phys. Chem. C 114 (2010) 22330–22337.
[41] C.G. Zhang, J. Dai, Z.P. Huo, X. Pan, L.H. Hu, F.T. Kong, Y. Huang, Y.F. Sui, X.Q. Fang, K.J. Wang, S.Y. Dai, Electrochim. Acta 53 (2008) 5503–5508.
[42] E. Stathatos, P. Lianos, S.M. Zakeeruddin, P. Liska, M. Gratzel, Chem. Mater. 15 (2003) 1825–1829.
[43] L.Y. Han, N. Koide, Y. Chiba, T. Mitate, Appl. Phys. Lett. 84 (2004) 2433–2435.
[44] J. Bisquert, F. Fabregat-Santiago, I. Mora-Sero, G. Garcia-Belmonte, S. Gimenez, J. Phys. Chem. C 113 (2009) 17278–17290.
[45] D.M. Li, H. Li, Y.H. Luo, K.X. Li, Q.B. Meng, M. Armand, L.Q. Chen, Adv. Funct. Mater. 20 (2010) 3358–3365.
[46] M.K. Wang, N. Chamberland, L. Breau, J.E. Moser, R. Humphry-Baker, B. Marsan, S.M. Zakeeruddin, M. Gratzel, Nat. Chem. 2 (2010) 385–389.